The Lipophilicity Patterns of Cyclodextrins and of Non-glucose Cyclooligosaccharides[1] *

FRIEDER W. LICHTENTHALER and STEFAN IMMEL
Institute of Organic Chemistry, Technical University of Darmstadt, D-64287 Darmstadt, Germany

Abstract. Computer-aided generation of the 3D-geometries and the contact surfaces for the cyclodextrins and cyclooligosaccharides composed of mannose, altrose, galactose, and fructose provide a lucid picture of their molecular architecture, most notably their cavity dimensions. The MOLCAD program's computation of the molecular lipophilicity patterns (MLPs), projected in color-coded form onto the respective contact surfaces, for the first time allow a detailed localization of hydrophobic and hydrophilic domains, which to a substantial degree determine the capabilities of these cyclooligosaccharides for inclusion complex formation.

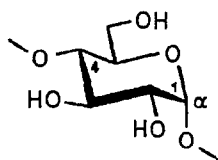**Key words:** lipophilicity pattern, cyclodextrins, non-glucose cyclooligosaccharides.

1. Introduction

The common, starch-derived cyclodextrins **4-6**, cyclic oligosaccharides composed of six, seven, or eight $\alpha(1\rightarrow4)$-linked D-glucopyranose units [2], have all been characterized by X-ray diffraction [3], thus unequivocally establishing their solid-state molecular geometries as depicted in Figure 1, together with their contact surfaces, shown as a dotted pattern [4, 5]. Of the 'small-ring cyclodextrins' **1-3**, which cannot be obtained from the action of *Bacillus macerans* amylase on starch, the cycloglucopentaoside **3** has yielded to chemical synthesis [6], and was shown by molecular modeling [7, 8] to exhibit a small cavity with only slight distortions of the glucose $^4C_1$ conformations. The cycloglucotetraoside **2** and its trimeric analog **1**, however, have no cavity (cf. Figure 1), and the pyranoid rings are forced into highly strained envelope conformations (E_1) [7];

---

* This account is based on an invited lecture presented by F. W. L. at the 8th International Cyclodextrin Symposium, Budapest, March 31 1996.

it is therefore unlikely that they will become available by chemical synthesis.

Small-ring cyclodextrins:

1	*cyclo*[D-Glc*p* α(1→4)]$_3$
2	*cyclo*[D-Glc*p* α(1→4)]$_4$
3	*cyclo*[D-Glc*p* α(1→4)]$_5$

Native cyclodextrins:

(α-CD)	**4**	*cyclo*[D-Glc*p* α(1→4)]$_6$
(β-CD)	**5**	*cyclo*[D-Glc*p* α(1→4)]$_7$
(γ-CD)	**6**	*cyclo*[D-Glc*p* α(1→4)]$_8$
(δ-CD)	**7**	*cyclo*[D-Glc*p* α(1→4)]$_9$
(ε-CD)	**8**	*cyclo*[D-Glc*p* α(1→4)]$_{10}$
(η-CD)	**9**	*cyclo*[D-Glc*p* α(1→4)]$_{12}$

Nomenclature: In accordance with the simplified designation recently proposed [7, 8], all cyclooligosac charides composed of glucose units are given the generic name cyclodextrin, irrespective of their intersaccharidic linkage, and specific names in accordance with present carbohydrate nomenclature. Thus, α-CD is a cyclo-α(1→4)-glucohexaoside, abbreviated *cyclo*[D-Glc*p* α(1→4)]$_6$, rather than a 'cyclomaltohexaose' which entails confusion as to the number of maltose residues (six ?) and the presence of a free anomeric center by the ending -ose.

Indications of the existence of larger cyclodextrins, i.e. those composed of nine, ten and more glucose units, had already been obtained 30 years ago [9], yet only recently were they isolated and unequivocally characterized: δ-CD (**7**) [10], ε-CD (**8**) [11], and η-CD (**9**) [12] with 9, 10 and 12 α-D-glucopyranosyl residues, respectively. Their gross molecular shape, however, is no longer dictated by the strict necessity for the glucose moieties to adopt a common tilt within the macrocycle; the 'straitjacket' becomes too wide, allows higher flexibility, i.e. different canting of the pyranoid rings and, hence, substantial puckering of the torus. The nine-glucose unit δ-CD (**7**), in the solid state [10a], adopts a bowl-shaped rather than a planar structure: four of the nine glucose units are distinctly canted with their primary 6-OH groups towards the cavity center, while the others line up almost perpendicular to the macrocyclic ring or are even inclined towards the opposite direction (cf. Figure 1). The 2-OH/3-OH aperture is opened much wider than the opposite 6-CH$_2$OH side, and the range for the tilt angle (τ = 77–141°) is unusually large [5]. The same holds true for ε-CD (**8**) with 10 glucose moieties in the macrocycle: the X-ray structure [11] reveals a boat form or U shape with an elliptical cavity, caused by two glucotrioside units – of identical shape and situated on opposite sides – linked by two equally identical, yet differently canted glucodiosides. Undoubtedly, the possibilities for the construction of further unusually puckered macrocyclic conformations will increase with cyclodextrins composed of more than 10 glucose units.

Cyclooligosaccharides composed of sugars other than glucose have gained considerable attention recently [8, 13–18]. As the cyclodextrins derive their name from dextrose, an early synonym for glucose, it is an obvious extension to bestow upon
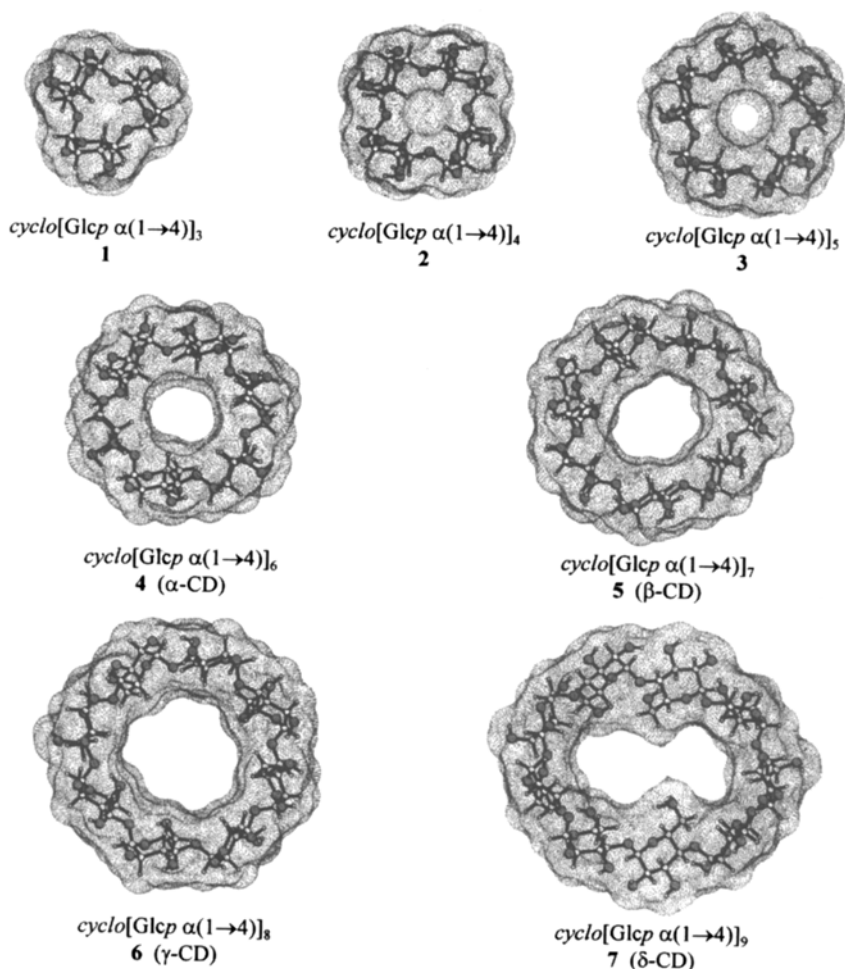
cyclo[Glc*p* α(1→4)]₃
1

cyclo[Glc*p* α(1→4)]₄
2

cyclo[Glc*p* α(1→4)]₅
3

cyclo[Glc*p* α(1→4)]₆
4 (α-CD)

cyclo[Glc*p* α(1→4)]₇
5 (β-CD)

cyclo[Glc*p* α(1→4)]₈
6 (γ-CD)

cyclo[Glc*p* α(1→4)]₉
7 (δ-CD)

Figure 1. Ball-and-stick model representations of the minimum-energy structures for the small-ring cyclodextrins **1–3**, generated by the PIMM91 force-field program [7, 8], and the X-ray-derived [3, 10] solid-state structures of **4–7** [4, 5], together with their contact surfaces, shown as a dotted pattern. Structures are shown perpendicular to the mean ring plane of the macrocycles and are viewed through the large opening of the conically shaped molecules, i.e. the 2-OH/3-OH sides of the pyranoid rings point towards the viewer, and the primary 6-CH₂OH groups away from him towards the back; oxygen atoms are shaded.

cyclooligosaccharides with mannose, altrose, galactose, fructose, and rhamnose units the generic name cyclomannins, cycloaltrins, cyclogalactins, cyclofructins, and cyclorhamnins, respectively [8]. Figure 2 depicts the molecular geometries, contact surfaces and cross section contours for the respective hexameric species generated by molecular modelling, revealing subtle differences in their cavity dimensions, α-cyclofructin being devoid of a cavity.

The well-documented ability of cyclodextrins to incorporate a wide variety of hydrophobic molecules into their cavities infers those cavities to be hydrophobic a priori. However, just how hydrophobic they are, and to what extent hydrophobic interactions between guest and host play a role in the formation of inclusion complexes, is an open question, since it has never been possible to quantify the individual terms involved, nor to assess where exactly the hydrophobic and hydrophilic surface regions are, and how far they extend from or into the cavity, respectively. While such questions are as yet quite elusive to exact experimental characterization [19], they yield to computer modeling via generation of the **molecular lipophilicity patterns** (MLPs) – an approach that provides a surprisingly lucid picture of the distribution of hydrophobic and hydrophilic 'patches' on the respective contact surfaces, particularly when transposed into a two-color-code representation: blue for hydrophilic, yellow for hydrophobic regions [4, 5, 7, 8]. The following account gives a review of the present state of our studies on this topic.

2. Materials and Methods

Calculation of the *molecular contact surfaces* [20] and the **molecular lipophilicity patterns** (MLPs) [21] was carried out by using the MOLCAD [22] molecular modeling program. Color-coded projection of the MLPs onto the corresponding contact surfaces was done by applying texture mapping strategies [23], using a two-color code graded into 32 shades, ranging from dark blue for the most hydrophilic areas to yellow for the most hydrophobic regions. Scaling of the hydrophobicity profiles was performed in arbitrary units and in relative terms for each molecule separately; no absolute values are displayed. Color graphics were photographed from the computer screen of a Silicon-Graphics workstation.

3. Results and Discussion

The lipophilicity patterns (MLPs) of α-, β-, and γ-CD (4–6) are depicted in Figure 4. They reveal the 2-OH/3-OH side of the macrocycles, i.e. the respective wider torus rim, to be distinctively hydrophilic as evidenced by the clearly defined blue areas (left entries). This is contrasted by hydrophobic (yellow) surface regions on

Figure 2. (opposite) Comparison of molecular geometries (ball-and-stick models), contact surfaces (shown in dotted form), and cross section contours of cyclooligosaccharides with six identical monosaccharide units each. To simplify their designation, all are given the prefix α – in analogy with α-cyclodextrin (α-CD, top left [7]), despite the fact that the linkage geometries in α-cyclofructin (bottom left [17]) and in α-cyclogalactin (bottom right [8] – which can easily be infered from the more precise abbreviations given – are different from that realized in α-CD. The cavity dimensions of α-cyclomannin [8] and its all–6-deoxy-L-analog α-cyclorhamnin are very similar (top center and right); α-cyclofructin has a disk-shaped molecular shape with an indentation only on either side [17]; the gross molecular structure of α-cycloaltrin (bottom center) [25] is derived from HTA simulations with an all-twist conformation of the pyranoid rings.
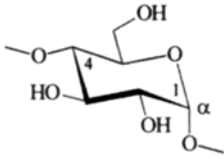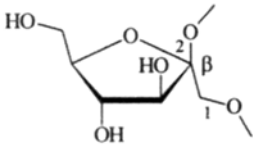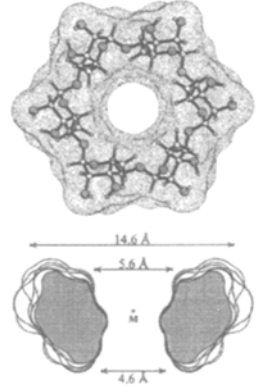
Cyclodextrins
cyclo[D-Glc*p* α(1→4)]₆
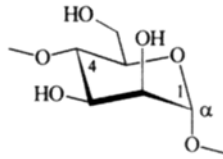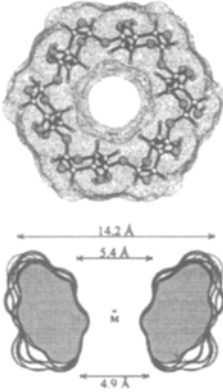
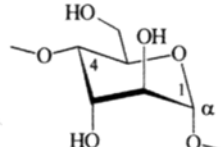**Cyclomannins**
cyclo[D-Man*p* α(1→4)]₆
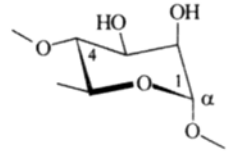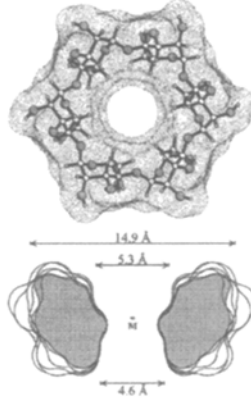
Cyclorhamnins
cyclo[L-Rha*p* α(1→4)]₆

Cyclofructrins
cyclo[D-Fru*f* β(1→2)]₆
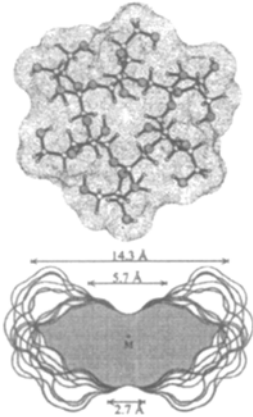
Cycloaltrins
cyclo[D-Alt*p* α(1→4)]₆
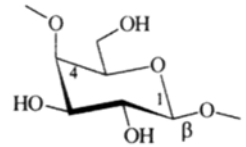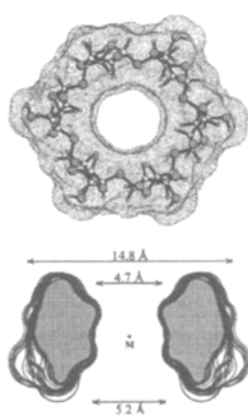
Cyclogalactins
cyclo[D-Gal*p* β(1→4)]₆
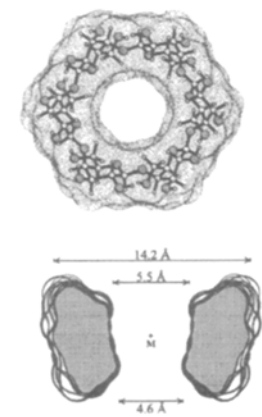
the opposite narrower opening made up of the 6-CH$_2$OH groups (Figure 4, center models), obviously caused by the close spatial arrangement of the 6-CH$_2$- and O$_5$-C$_5$-H$_5$-fragments of the glucose residues [5]. Out of the calculated total surface area of $\approx$120 Å^2 per glucose unit (α-CD: 720, β-CD: 845, and γ-CD: 960 Å^2), only approximately 10–15% contributes to the inner surface of the central cavity (α-CD: 85, β-CD: 105, and γ-CD: 140 Å^2), yet the highest hydrophobicity is invariably to be found within this inner area of the molecular surface. Most notably, however – and this is vividly illustrated by the side view MLPs in bisected form (Figure 4, right entries) – *not the entire cavity surface areas are hydrophobic*, but only those regions in the narrower half of the cone structures, and these extend well out of the cavities towards the primary hydroxyl faces. Accordingly, the widespread view that only the cavity of the cyclodextrins is hydrophobic, or that "two hydrophilic faces surround a hydrophobic cavity [24]", is likely to be subject to revision.

In a similar fashion, the preferred conformations, the contact surfaces which reveal the cavity proportions, and the MLPs of non-glucose cyclooligosaccharides can be computed and evaluated in terms of their capabilities to form inclusion complexes.

The α-*cyclomannin*, which has been synthesized [13], but in such minute amounts as to exclude studies on its inclusion complex behavior, has a backbone structure similar to α-CD (cf. Figure 2), indicating that inversion of the glucosyl-2-OH in the pyranoid rings entails no principal changes, the somewhat smaller torus height being only a minor effect [8]. The cavity dimensions resemble those of α-CD, as do the MLP profiles (Figure 5, top entries), except for the finding that the outer surface areas of α-cyclomannin are more thoroughly hydrophilic than the ones in α-CD, obviously due to the more clearly cavity-localized hydrophobic regions (cf. side view in Figure 5). *In toto*, its behavior towards inclusion complex formation should be very similar to α-CD [8].

For the α-*cycloaltrin*, which has recently become accessible from α-CD by a straightforward three- step synthesis [15b], one would expect the altropyranoid rings to either adopt the all-$^4C_1$ (**A**) or the all-$^1C_4$ conformation (**B**), or – in aqueous solution more likely – a dynamic equilibrium between the two conformational extremes, i.e. **A** $\rightleftharpoons$ **B** (cf. Figure 3).

For vacuum boundary conditions, the all-*twist* or all-*'skew boat'* form **C** emerged from high temperature annealing (HTA) simulations [25] as the energetically most favorable one. In **C**, the steric constraints imposed on form **A** by the *syn*-1,3-diaxial interactions between the intersaccharidic oxygen (O^1) and O^3, and the congestion exerted by the six axial 3-OH projecting into the cavity, are released, yet it also causes the tilt of the altropyranose units to be inverted: the primary hydroxyl face becomes the larger opening, the torus rim carrying the secondary hydroxyls the smaller one (cf. cross-cuts in Figure 2). However, the alternative conical shape has only minor consequences for the lipophilicity distribution, as the secondary hydroxyl face is distinctly hydrophilic (blue, cf. Figure 5, center entries) versus a
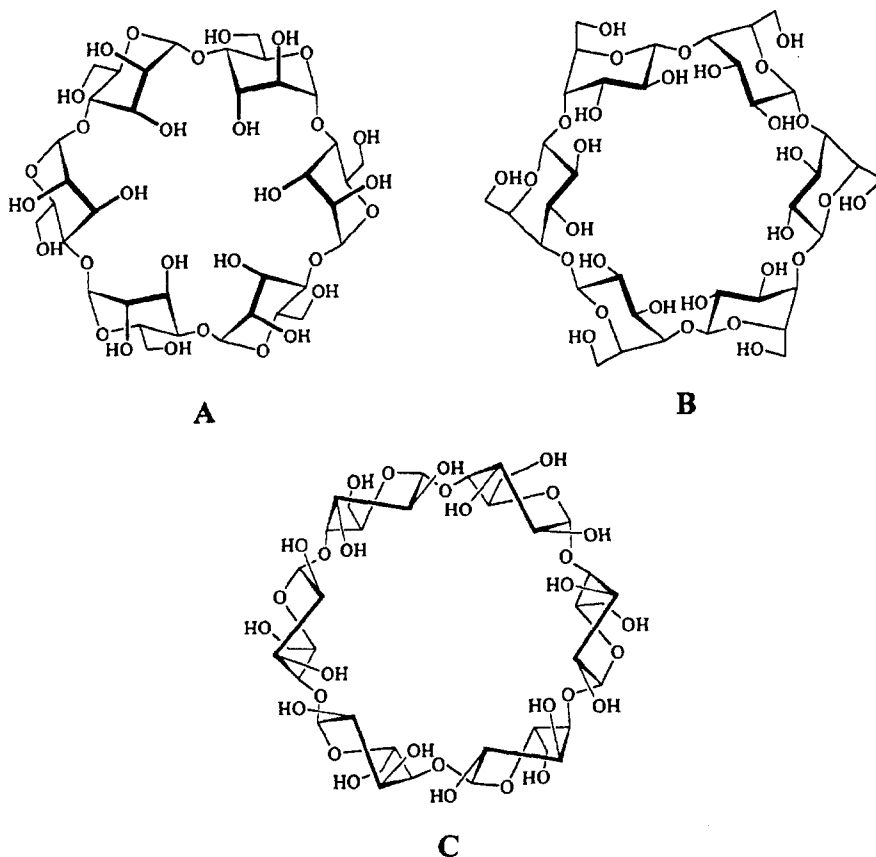
Figure 3. α-Cycloaltrin with different conformations of the pyranoid ring: the *all-$^4C_1$-form* **A**, which is encumbered with *syn*-1,3-diaxial interactions between the 3-OH and the intersaccharidic 1-oxygen, as well as with the steric congestion created by the six axial 3-OH sticking into the center cavity; the alternate *all-$^1C_4$ form* **B** appears to be less burdened by steric constraints, whilst the *all-twist form* **C** represents a conformational arrangement between the two extremes **A** and **B**. High-temperature annealing (HTA) simulations on the isolated molecules (i.e. for vacuum boundary conditions) led [26] to the *all-twist* (*skew boat*) geometry **C** as the energetically most favorable arrangement; in aqueous solution a dynamic equilibrium **A** $\leftrightharpoons$ **B** or a solvated intermediate form of type **C** appears to be likely.

hydrophobic (yellow) cavity area reaching out over the wider torus rim lined by the six CH$_2$OH groups [25].

While this *all-twist* form **C** of α-cycloaltrin, if proved to be prevalent in solution, would be the first cyclooligosaccharide with *'inverse conicity'*, there are other forms conceivable, a most fascinating one being an 'internal hybrid form' between **A** and **B**, i.e. a continuous succession of $^4C_1$ and $^1C_4$ altropyranoid chairs around the macrocycle. It appears not unlikely that this hybrid form is adopted in the solid state.
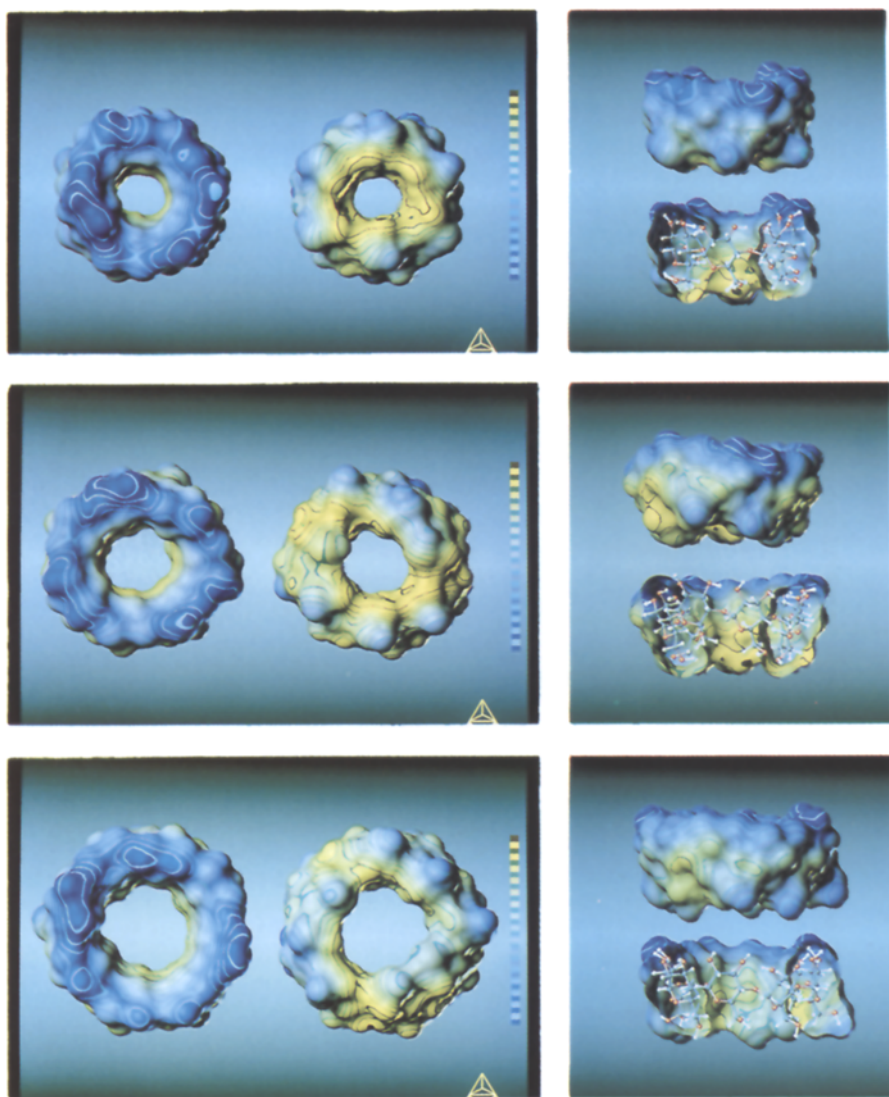
Figure 4. MOLCAD program-generated molecular lipophilicity patterns (MLPs), projected onto the respective contact surfaces (cf. Figure 1) of α-CD (**4**, top entry), β-CD (**5**, center), and γ-CD (**6**, bottom). The pictures on the left are viewed through the larger openings of the conically shaped molecules thus exposing the intensively hydrophilic (blue) 2-OH/3-OH side, whereas the representations in the middle depict the opposite side, i.e. the smaller opening with the 6-CH$_2$OH groups facing the viewer, thereby clearly exposing the hydrophobic (yellow) surface areas. The side view MLPs on the right, each in closed and bisected form, are oriented such that the 2-OH/3-OH side is aligned upward (larger opening of the torus) and the 6-CH$_2$OH groups are pointing down (smaller aperture). The similarities in the distribution of hydrophilic (blue) and hydrophobic (yellow) surface areas – most notably on the inside regions of the cavities of α-, β-, and γ-CD – are clearly apparent [5].

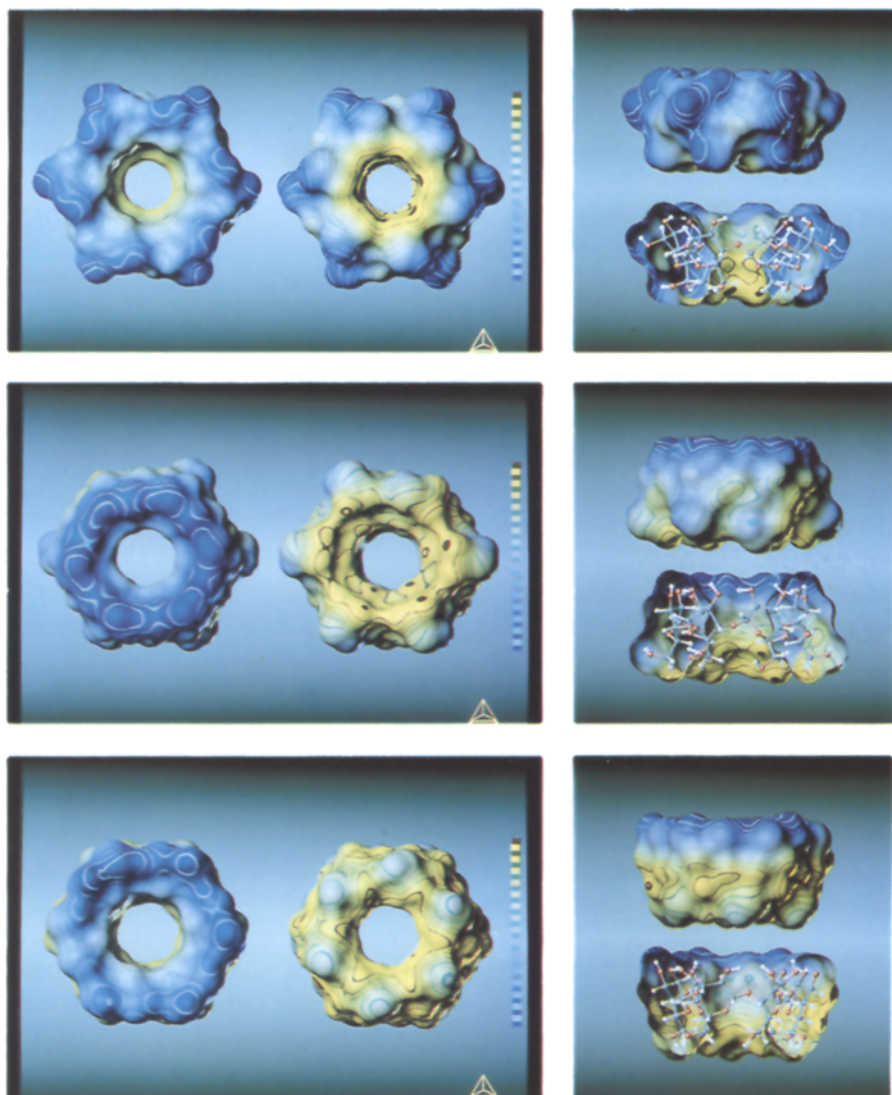*Figure 5.* Molecular lipophilicity patterns (MLPs) for α-cyclomannin (top, cyclo-α(1→4)-mannohexaoside), α-cycloaltrin (cyclo-α(1→4)-altrohexaoside, center), and α-cyclogalactin (cyclo-β(1→4)-galactohexaoside, bottom) [8], in order from left to right: hydrophilic side (blue, 2-OH/3-OH face oriented to the viewer) → hydrophobic primary hydroxyl face (yellow) → closed and bisected side views.

In the case of *α-cyclogalactin*, requiring $\beta(1\rightarrow4)$-linkages to enable a CD-analogous cyclooligosaccharide, the pyranoid ring oxygens are directed towards the inside, entailing a cavity less congested (than in α-CD) by hydrogen atoms, hence wider by about 20%, and of more tube-like shape [8] (Figure 2). This *'inside-turned-out'* cyclic ribbon of pyranoid chairs is also evidenced in a lipophilicity distribution inverse to that of α-CD: substantially enlarged hydrophobic surface areas at the primary CH₂OH face, extending significantly out of the cavity over the rim towards the outside of the macrocycle (Figure 5, bottom entries) [8]. Accordingly, α-cyclogalactin – unlike α-CD – is surmised to be barely soluble in water, which will facilitate its isolation when the efforts towards its synthesis [26] materialize.

The inulin-derived *α-cyclofructin*, consisting of six $\beta(1\rightarrow2)$-linked fructofuranose units adding up to a crown ether backbone, reveals a contact surface topography devoid of an inner cavity [4, 17], and an MLP profile (Figure 6, top) with front-side/back-side separation of hydrophilic and hydrophobic areas. Due to the location of three fructosyl-oxygens (1-O, 3-OH, and 4-OH) on the same ('front') side of the disk-shaped molecule, this surface region is distinctly hydrophilic. The opposite side holds the 1-CH₂, 6-CH₂ and 5-CH fragments, and accordingly entails a distinctly hydrophobic 'back-side', the indentation in its center being open for potential binding with complementary guests, albeit not in an inclusion type fashion [17].

O-Alkylated or *O*-acylated derivatives of the cyclodextrins, as well as those where OH groups have been replaced by hydrogen, halogen, or amino functionalities, may also be subjected to this methodology, providing lucid pictures of their hydrophobicity/hydrophilicity distributions. Thus, the per-*O*-methylated α-CD and β-CD – not unexpected due to the 'lipophilization' of their OH-groups by methylation – show lipophilicity patterns inverse to that of their parent cyclodextrins: hydrophilic central cavities and the most hydrophobic surface regions located at the torus rims made up of the 2-OMe and 3-OMe at one side, and the 6-CH₂OMe moieties at the other [1]. A variety of experimental findings can be rationalized on the basis of the opposed lipophilicity profiles, such as for example the opposite orientation of benzaldehyde, *p*-nitrophenol, and 3-iodopropionic acid in the cavities of α-CD and of per-*O*-methyl-α-CD. Thus, the notion is substantiated that the operation of dispersive interactions between guest and CD-host cavities play a more dominant role in inclusion complex formation than has hitherto been appreciated.

The computational methodology applied to the 'empty' cyclooligosaccharides can, of course, be put to use for unraveling the lipophilicity patterns of their inclusion complexes, particularly for exploring the degree of conformity of hydrophobic and hydrophilic areas at the interface between guest and host [27]. Impressive examples are the complexes of β-CD with adamantane-1-carboxylic acid and its 1-methanol derivative (Figure 6, center) [27]: in the solid state, either complex is characterized by head-to-head arranged β-CD dimers formed through an intense hydrogen bonding network between the secondary OH-groups of two CD tori,
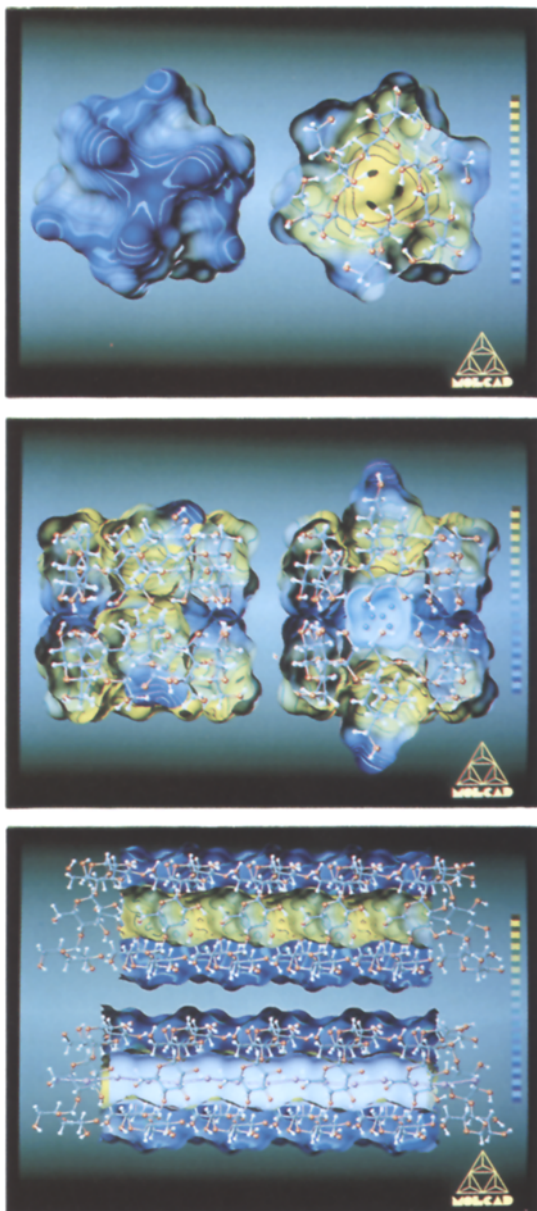
Figure 6. *Top:* Molecular lipophilicity pattern for α-cyclofructin (cyclo-$\beta(1\rightarrow2)$-fructohexaoside) [17]. *Center:* Inclusion complex of β-cyclodextrin with adamantane-1-carboxylic acid (left) and adamantane-methanol (right). While the carboxylic acid residue is fully immersed in the cavities, the hydroxymethyl group projects outwards, due to water molecules being locked in the center of the double cavity (two H_2O distributed over six crystallographic positions) [27]. *Bottom:* The single-stranded V_H-amylose with six glucose units per turn, in a section of ≈30 Å length; the half-opened model unveils the distinctly hydrophobic center channel, into which iodine is incorporated to form the dark-blue amylose-iodine complex [4, 30].

with the highly hydrophobic adamantyl moieties facing each other in the 'double' cavities. In the 1-carboxylic acid case, the guest is either fully immersed in the cavity with the hydrophilic head group located at the primary hydroxyl side, or is only included with its adamantyl portion (Figure 6, center left), both insertion modes providing an ideal disposition for the carboxyl group to engage in hydrogen bonding to CD-hydroxyl groups of the next dimer, or to water. In the adamantane-1-methanol case, the molecular assembly is basically similar with respect to the dimer formation, yet distinctly different in terms of the depths of immersion of the intensely hydrophobic adamantane residues. The 1-methanol group protrudes from either end, leaving empty space on the hydrophilic middle ribbon of the cavity, which is filled with two water molecules (Figure 6, center right), thereby achieving an optimum match of hydrophobic and hydrophilic surface regions [27].

The MOLCAD program methodology was also used to generate the contact surface and MLP profile for the V_H-amylose portion of starch, which on the basis of X-ray diffraction studies [28] forms a single-stranded left-handed helix with six glucose units per turn. As is clearly apparent from the color-coded representations in Figure 6 (bottom entries), the outside surface regions of V_H-amylose are intensely hydrophilic (blue) – corroborating its solubility in water – while its center channel is decisively hydrophobic (yellow) [4, 29]. This distinctive *'inside-outside'* separation of hydrophobic and hydrophilic domains preconditions the incorporation of iodide/iodine into the channel as a successive linear chain of I_2/I_3^- molecules [30], generating the dark-blue amylose–iodine complex [30], which thereby becomes conceptually understandable [4, 29].

Acknowledgment

References

1. 'Molecular Modelling of Saccharides', Part 14. – Part 13: S. Immel, and F.W. Lichtenthaler: 'Permethylated α- and β-CD: cyclodextrins with inverse hydrophobicity', *Starch/Stärke*, **48**, 225–232 (1996). This account is based on an invited lecture presented by F.W. L. at the 8th International Cyclodextrin Symposium, Budapest, March 31, 1996.
2. W. Saenger: 'Cyclodextrin Inclusion Compounds in Research and Industry', *Angew. Chem. Int. Ed. Engl. 19*, 344–362 (1980). J. Szejtli: *Cyclodextrins and their Inclusion Complexes*, Akademia Kiado, Budapest, 1982. *Cyclodextrin Technology*, Kluwer Academic Publishers, Dordrecht, 1988. G. Wenz: 'Cyclodextrins as Building Blocks for Supramolecular Structures', *Angew. Chem. Int. Ed. Engl. 33*, 803–822 (1994), and literature cited therein.
3. K. Harata: 'Recent Advances in the X-ray Analysis of CD Complexes', in: J.L. Atwood, J.E.D. Davies and D.D. MacNicol (eds.), *Inclusion Compounds*, Oxford University Press, Oxford, **5**, 311–344 (1991).

4. F.W. Lichtenthaler, and S. Immel: 'Computer Simulation of Chemical and Biological Properties of Sucrose, the Cyclodextrins, and Amylose', *Internat. Sugar J.* **97**, 12–22 (1995).

5. F.W. Lichtenthaler, and S. Immel: 'On the Hydrophobic Characteristics of Cyclodextrins: Computer-aided Visualization of Molecular Lipophilicity Patterns', *Liebigs Ann. Chem.* **27–37** (1996).

6. T. Nakagawa, K. Ueno, M. Kashiwa, and J. Watanabe: 'Preparation of a Novel Cyclodextrin Homologue with d.p. Five', *Tetrahedron Lett.* **35**, 1921–1924 (1994).

7. S. Immel, J. Brickmann, and F.W. Lichtenthaler: 'Small-ring Cyclodextrins: Their Geometries and Hydrophobic Topographies', *Liebigs Ann. Chem.* 929–942 (1995).

8. F.W. Lichtenthaler, and S. Immel: 'Cyclodextrins, Cyclomannins, and Cyclogalactins with Five and Six $(1{\rightarrow}4)$-linked Sugar Units: A Comparative Assessment of their Conformations and Hydrophobicity Potential Profiles', *Tetrahedron Asymmetry*, **5**, 2045–2060 (1994).

9. D. French, A.O. Pulley, J.A. Effenberger, M.A. Rougvie, and M. Abdullah: 'The Schardinger Dextrins: Molecular Size and Structure of the δ-, ε-, ζ-, and η-dextrins', *Arch. Biochem. Biophys.* **111**, 153–160 (1965).

10. T. Fujiwara, N. Tanaka, and S. Kobayashi: 'Structure of δ-cyclodextrin·13.75 H_2O', *Chem. Lett.* 739–742 (1990). I. Miyazawa, H. Ueda, H. Nagase, T. Endo, S. Kobayashi, and T. Nagai: 'Physicochemical Properties and Inclusion Complex Formation of δ-CD', *Europ. J. Pharm. Sci.* **3**, 153–162 (1995).

11. H. Ueda, T. Endo, H. Nagase, S. Kobayashi, and T. Nagai: 'Isolation, Purification, and Characterization of ε-CD', *8th Internat. Cyclodextrin Symp., Budapest*, Abstract 1-p 12 (1996).

12. T. Endo, H. Ueda, S. Kobayashi, and T. Nagai: 'Isolation, Purification and Characterization of Cyclomalto-dodecaose (η-CD)', *Carbohydr. Res.* **269**, 369–373 (1995).

13. M. Mori, Y. Ito, and T. Ogawa: 'A Highly Stereoselective and Practical Synthesis of Cyclomannohexaose', *Carbohydr. Res.*, **192**, 131–146 (1989). M. Mori, Y. Ito, J. Izawa, and T. Ogawa: 'Stereoselectivity of Cycloglycosylation in *Manno*oligose Series Depends on Carbohydrate Chain Length: Synthesis of *Manno*-isomers of β- and γ-cyclodextrins', *Tetrahedron Lett.* **31**, 3191–3194 (1990).

14. M. Nishizawa, H. Imagawa, Y. Kan, and H. Yamada: 'Synthesis of Cyclo-L-rhamnohexaose by a Stereoselective Thermal Glycosylation', *Tetrahedron Lett.* **32**, 5551–5554 (1991). M. Nishizawa, H. Imagawa, E. Morikuni, S. Hatekayama, H. Yamada: 'Synthesis of Cyclo-L-rhamnopentaose', *Chem. Pharm. Bull.*, **42**, 1356–1365 (1994).

15. (a) K. Fujita, H. Shimada, K. Ohta, Y. Nogami, K. Nasu, and T. Koga: 'β-Cycloaltrin: A Cyclooligosaccharide Consisting of Seven $\alpha(1{\rightarrow}4)$-linked Altropyranoses', *Angew. Chem. Int. Ed. Engl.* **34**, 1621–1622 (1995). (b) Y. Nogami, K. Fujita, K. Ohta, K. Nasu, H. Shimada, C. Shinohara, and T. Koga: 'CD-derived Cycloaltrins Made Up from $\alpha(1{\rightarrow}4)$-linked Altropyranoses', *8th Internat. Cyclodextrin Symp., Budapest*, Abstract 1-p 10 (1996).

16. M. Sawada, T. Tanaka, Y. Takai, T. Hanafusa, T. Taniguchi, M. Kawamura, and T. Uchiyama: 'Crystal Structure of Cycloinulohexaose from Inulin', *Carbohydr. Res. 217*, 7–17 (1991).

17. S. Immel, and F.W. Lichtenthaler: 'The Electrostatic and Lipophilic Potential Profiles of α-cyclofructin: Computation, Visualization and Conclusions', *Liebigs Ann. Chem.*, 39–44 (1996).

18. P.R. Ashton, C.L. Brown, S. Menzer, S.A. Nepogodiev, J.F. Stoddart, D.J. Williams: 'Syntheses and Structural Porperties of Cyclo[$(1{\rightarrow}4)$-α-L-rhamnosyl-$(1{\rightarrow}4)$-α-D-mannosyl]trioside and -tetraoside', *Chem. Eur. J.* **2**, 580–591 (1996).

19. W. Blokzijl, and J. B. F. N. Engberts: 'Hydrophobic Effects, Opinions and Facts', *Angew. Chem. Int. Ed. Engl.* **32**, 2045–2060 (1993).

20. F.M. Richards: 'Areas, Volumes, Packing, and Protein Structure', *Ann. Rev. Biophys. Bioeng.* **6**, 151–176 (1977); *Carlsberg. Res. Commun.* **44**, 47–63 (1979). M.L. Connolly: 'Analytical Molecular Surface Calculation', *J. Appl. Cryst.* **16**, 548–558 (1983); *Science* **221**, 709–713 (1983).

21. W. Heiden, G. Moeckel, J. Brickmann: 'A New Approach to Analysis and Display of Local Lipophilicity/Hydrophilicity Mapped on Molecular Surfaces (MLP)', *J. Comput.-Aided Mol. Des.* **7**, 503–514 (1993).

22. J. Brickmann: *MOLCAD – MOLecular Computer Aided Design*, Technische Hochschule Darmstadt. The major part of the MOLCAD program is included in the SYBYL package of TRIPOS

Associates, St. Louis, USA (1992). J. Brickmann: 'Molecular Graphics – How to See a Molecular Scenario with the Eyes of a Molecule', *J. Chim. Phys. 89*, 1709–1721 (1992). J. Brickmann, T. Goetze, W. Heiden, G. Moeckel, S. Reiling, H. Vollhardt, and C.D. Zachmann: 'Interactive Visualization of Molecular Scenarios with MOLCAD/SYBYL', in: J.E. Bowie (ed.), *Data Visualization in Molecular Science – Tools for Insight and Innovation* Addison-Wesley Publ., Reading, Mass. pp. 83–97 (1995).

23. M. Teschner, C. Henn, H. Vollhardt, S. Reiling, and J. Brickmann: 'Texture Mapping, a New Tool for Molecular Graphics', *J. Mol. Graphics* **12**, 98–105 (1994).

24. H. Parrot-Lopez, C.-C. Ling, P. Zhang, A. Baszkin, G. Albrecht, C. de Rango, and A.W. Coleman: 'Self-assembling Systems of Amphiphilic per-6-amino-β-cyclodextrin 2,3-dialkyl Ethers', *J. Am. Chem. Soc.* **114**, 5479–5480 (1992).

25. F.W. Lichtenthaler, S. Immel, and G.E. Schmitt: unpublished results.

26. M. Oberthür: *Aufbau $\beta(1{\rightarrow}4)$-verknüpfter Galactooligosaccharide*, Diplomarbeit, Techn. Hochschule Darmstadt, (1995).

27. F.W. Lichtenthaler, and S. Immel: 'Towards Understanding the Formation and Stability of Cyclodextrin Inclusion Complexes: Computation and Visualization of their Lipophilicity Patterns', *Starch/Stärke*, **48**, 145–154 (1996).

28. G. Rappenecker, and P. Zugenmaier: 'Detailed Refinement of the Crystal Structure of V_H-amylose', *Carbohydr. Res.* **89**, 11–19 (1981).

29. S. Immel, and F.W. Lichtenthaler: 'The Hydrophobic Topographies of Amylose and its Blue Iodine Complex', to be published.

30. T.L. Bluhm, and P. Zugenmaier: 'Detailed Structure of the V_H-Amylose-iodine Complex: A Linear Polyiodine Chain', *Carbohydr. Res.* **89**, 1–10 (1981).